

Research Article

Additive Manufacturing of Silencers with Microperforates

Jukka Tanttari,¹ Erin Komi,² Antti Hynninen ,² Heikki Isomoisio,¹ Seppo Uosukainen,² Virpi Hankaniemi,³ and Mikko Matalamäki³

¹VTT Technical Research Centre of Finland Ltd., FI-33101, Tampere, Finland

²VTT Technical Research Centre of Finland Ltd., FI-02044, Espoo, Finland

³Wärtsilä Finland Ltd., Energy Solutions, FI-65101, Vaasa, Finland

Correspondence should be addressed to Antti Hynninen; antti.hynninen@vtt.fi

Received 28 June 2018; Revised 25 September 2018; Accepted 30 September 2018; Published 14 October 2018

Guest Editor: Ping Xiang

Copyright © 2018 Jukka Tanttari et al. This is an open access article distributed under the Creative Commons Attribution License, which permits unrestricted use, distribution, and reproduction in any medium, provided the original work is properly cited.

A microperforated panel (MPP) is generally defined as a perforated plate, in which the impedance of below one millimetre perforations is dominated by viscous losses. Using MPPs in duct and silencer applications, target is to maximize transmission loss (TL) by choosing proper surface impedance parameters. Additive manufacturing (AM) has recently reduced conventional design limitations and enabled fast prototyping of complex shaped structures. MPP-based model scale silencers can be printed within reasonable time, price, and accuracy. In this paper, design and validation of AM silencers with MPPs are studied. First, the theoretical background of MPP acoustics is summarized. Second, feasible parameters for a MPP absorber for a certain tuning frequency are sought numerically using acoustic finite element method (FEM). Third, several test MPPs are prototyped and their acoustic properties are measured. Finally, MPP silencers are simulated using different approaches and the results are compared against experiments.

1. Introduction

A microperforated panel (MPP) is generally defined as a perforated plate, in which the impedance of a hole is dominated by viscous losses [1, 2]. In practice, this means that the diameters of the holes are below one millimetre and combined area of the holes is 0.5...4% of the total area of the panel. From an acoustic point of view, the MPP performs as a stiff surface with suitable acoustic resistance and low mass reactance.

There are two distinct MPP applications: (1), room acoustic applications, where high absorption coefficient is the target, and (2), duct and silencer applications, where surface impedance maximizing transmission loss (TL) is the target.

MPP silencers can be further divided into Cremer silencers and modal filter silencers [3–6]. In the first case, the aim is to create suitable (small) impedance to the silencer passage surfaces. A Cremer silencer typically works best at the plane wave region. They have high TL (peak up to 80 dB) at relatively narrow frequency band. The frequency of peak TL is called the tuning frequency.

In modal filter silencers, thin MPPs with predominantly resistive impedances are used and the MPPs are

placed on the duct cross section to locations of high particle velocity. The modal filter concept is aimed for, and works best, in case higher order propagating modes are important. Modal filter silencers typically have moderate TL at a relatively broad frequency band at high frequencies.

In case of a Cremer silencer, the value of optimal impedance depends on frequency, duct dimensions, and the order of the propagating waveguide mode. Value of the absorption coefficient may be much smaller than one. Kabral et al. [7] studied the relation of impedance and maximum TL in Cremer silencer in depth. Cremer and modal filter silencers are depicted in Figure 1. In the present paper, Cremer silencers are the principal interest.

Resistance and reactance of the fluid volume in the hole are usually tuned using the diameter of holes, thickness of the panel, perforation ratio and depth of the backing cavity. Ideally, the air gap (backing cavity depth) behind the MPP creates a locally reacting surface [3–7].

A Cremer silencer works best in case the acoustic reaction of the MPP surface is local. In local reaction condition, sound field is uniform over the MPP-backing cavity junction

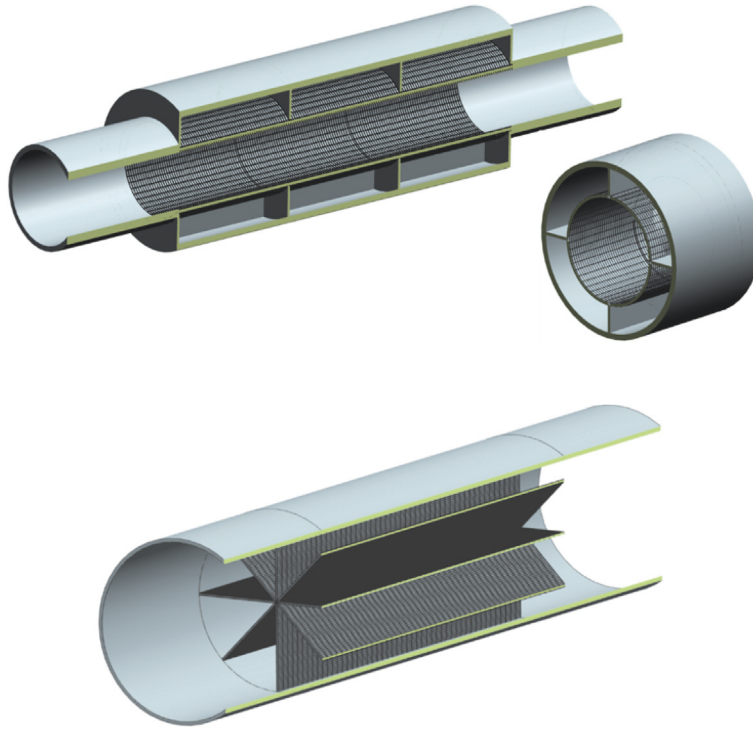


FIGURE 1: Typical MPP silencer constructions. Top: Cremer silencer. Bottom: modal filter silencer. Hatch patterned surfaces depict MPPs.

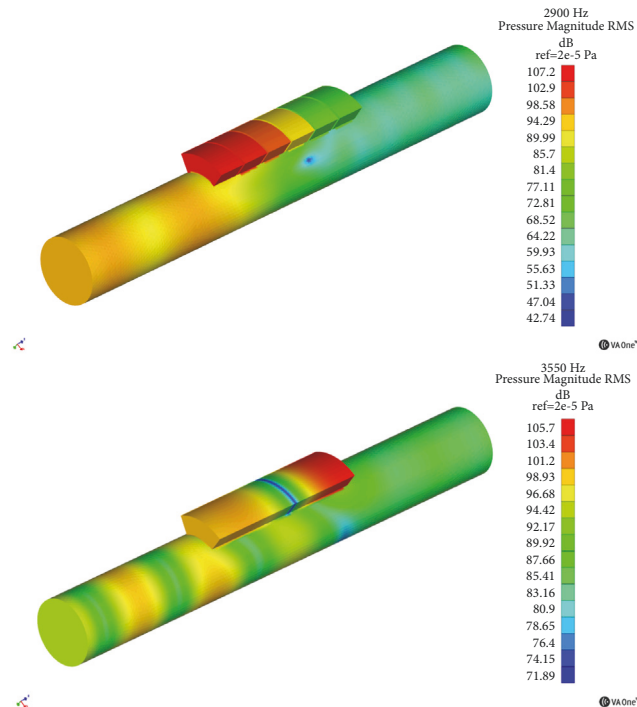


FIGURE 2: Sound pressure distribution in Cremer silencers. Acoustic excitation on the left hand side. Top: local reaction with 6 cavities, each 15 mm long; max. TL 30 dB at 2900 Hz. Bottom: extended reaction with one cavity 90 mm long; max. TL 8.5 dB at 3550 Hz.

surface, the particle velocity in MPP hole is in the normal direction and the sound field is uniform in the cavity. To maintain this in practice, lateral dimensions of the backing cavities should be much smaller than half wavelength at

the frequency of interest. Nonlocal reaction is also called extended reaction. As an example, sound pressure distributions in case of local and extended reactions are depicted in Figure 2.

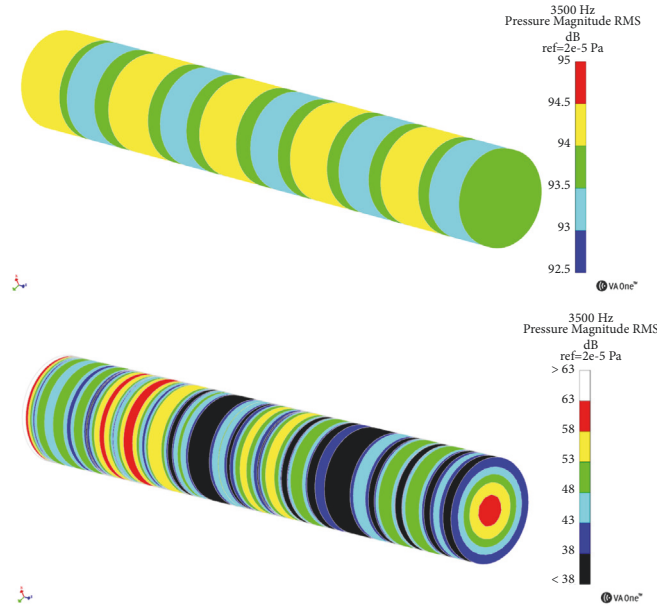


FIGURE 3: Sound pressure distribution in a Cremer silencer duct (length 240 mm, diameter 34.8 mm) excited at left end using sound pressure level of 94 dB. Top: rigid duct wall. Bottom: locally reacting duct surface; tuning frequency 3500 Hz. Note that the scale is different, because the incident wave does not propagate well. It decays over 40 dB in the first 50 mm.

Sound pressure distribution in a duct at tuning frequency is depicted in Figure 3. The fundamental plane wave mode, having a constant sound pressure over the cross section, does not propagate well, because the sound pressure decreases towards the surface of the duct wall.

Cremer silencers do not always perform as expected. The main reasons for performance anomalies are (1) leaks between backing cavities, (2) cavities with too large lateral dimensions (extended reaction), and (3) unsuitable MPP impedance.

Yang et al. [8] studied effect of drainage slots on performance of acoustic liners backed with honeycomb structure. In a series of experiments, it was shown that drainage slots (i.e., holes between backing cavities) had a very clear effect on TL peak frequency. Also, the width of the TL peak varied. In that case, the lateral dimensions of the honeycomb cells were only approx. 1/15 of wavelength, so the silencer performance did not break down and a local reaction could be assumed.

Allam and Åbom [9] studied a splitter type Cremer silencer. The lateral dimensions of backing cavities were altered. Cavities of 50 x 80 mm produced a TL of over 30 dB at approx. 1500 Hz. With large cavities, 160 x 240 mm this valued dropped to approx. 15 dB and with 500 x 1000 mm to 10 dB. Same time TL became more broadband. It has also been demonstrated in [6] that a porous (i.e., leaking) dividing walls between backing cavities has a distinct effect on TL.

Additive manufacturing (AM) has recently reduced conventional design limitations and enabled fast prototyping of complex shaped structures. Model scale silencers can be printed within reasonable time and price. Concerning MPPs, holes of $\varnothing=0.3$ mm are printable with typical stereolithography (SLA) printers.

Kabral et al. [10] demonstrated use of AM/3D Printing/Rapid Prototyping in producing MPP test silencers. In

that case, only the casing was printed. MPP part was a prefabricated commercial product. Liu et al. [11] used 3D printing to produce MPP specimen with 0.6 mm holes for impedance measurements. The hole geometries were not diagnosed, but measured absorption coefficients matched well with predicted values. Values of impedances were not shown in the paper.

In this paper, design and validation of additive manufactured Cremer silencers with MPPs are studied. First, the theoretical background of MPP acoustics is summarized. Second, feasible parameters for a MPP absorber for a certain tuning frequency are sought numerically using acoustic finite element method (FEM). Third, several test MPPs are prototyped and their acoustic properties are measured. Finally, MPP silencers are simulated using different approaches and the results are compared against experiments.

2. Acoustic Performance of MPP Absorbers

When a MPP is backed with a cavity (air gap) of depth D , impedance of the cavity (z_{CAV}) is added to the MPP impedance (z_{MPP}):

$$z = z_{MPP} + z_{CAV} = z_{MPP} - j \cot \frac{\omega D}{c_0}, \quad (1)$$

where ω is the angular frequency and c_0 is the speed of sound. The strategy to get a good silencer design is to create a system where the imaginary part is small or close to zero. This is not easy to arrange without a gap resonance condition. Typically the first (lowest) resonance is the mass-spring resonance (i.e., Helmholtz-type) as the higher resonances are associated with standing waves in the gap. Note that equation (1) assumes a one-dimensional sound field. This condition is not

TABLE 1: Three MPP-gap options tuned to 3500 Hz.

Option	MPP parameters			Cavity/Gap	
	Perforation ratio σ [%]	MPP thickness t [mm]	Hole diameter d [mm]	Perforate constant in air at 3500 Hz	Backing cavity depth D [mm]
A	5.0	1.0	0.3	5.8	8.0
B	7.0	1.5	0.4	7.7	8.0
C	10	1.5	1.0	19	9.7

Note that option C is, strictly speaking, not MPP because hole diameter is 1 mm.

necessarily fulfilled if the cavity has large lateral dimensions. The optimal wall impedance for an infinite rectangular duct was derived by Cremer [12]. Using the same principles, Tester [13] derived the optimal wall impedance for the plane wave modes in circular ducts with radius R as

$$z_{N,Opt} = (0.88 - 0.38i) \frac{\omega R}{\pi c_0}. \quad (2)$$

For a circular duct with 0.05 m diameter, the optimal normalized impedance at 500 Hz is $0.064 - 0.028i$, corresponding to absorption coefficient of approx. 0.23.

The specific acoustic impedance of a short tube (single MPP hole) is defined as

$$z_{MPP} = \frac{\Delta p}{u}, \quad (3)$$

where Δp is the pressure difference over the MPP thickness, and u is the average particle velocity in the hole. When using (3) it is implicitly assumed that the fluid is moving as a rigid mass in the hole; i.e., its compression is not taken into account. For very high frequencies this might be inaccurate.

The impedance z_{MPP} can be determined experimentally using an impedance tube. The values of $\text{Re}(z_{MPP})$ (resistance) and $\text{Im}(z_{MPP})$ (reactance) are different for holes of different shape, e.g., for circular holes or slits. It is also known that a grazing flow has influence and that high particle velocity inside the perforation has an effect on these values.

The most well-known way to predict the impedance of circular holed MPP is the formulation by Maa [1]:

$$z_{MPP} = \frac{32\eta t}{\sigma \rho c_0 d^2} \left(\sqrt{1 + \frac{\chi^2}{32}} + \frac{\sqrt{2} \chi d}{8t} \right) + \frac{j\omega t}{\sigma c_0} \left(1 + \frac{1}{\sqrt{9 + \chi^2/2}} + \frac{0.85d}{t} \right), \quad (4)$$

where η is the coefficient of the kinematic viscosity, t is the thickness of the MPP, σ is the perforation ratio, ρ is the density, d is the hole diameter, and the perforate constant is

$$\chi = \frac{d}{2} \sqrt{\frac{\omega \rho}{\eta}}. \quad (5)$$

Optimal values of χ for high absorption coefficient (i.e., room acoustic applications) are near one; i.e., the boundary layer fills the hole completely. This ensures that the movement of air in the hole is resistive. Values of χ much smaller than one lead to overly small holes and resistance too high for acoustic applications.

Very large values of χ indicate that the hole is not very resistive; i.e., it does not absorb sound due to a viscous friction process. Relatively high (between 2 and 20, say) values of χ are feasible in silencer applications.

3. Feasible MPP Parameters for 3500 Hz Tuning Frequency

The plan was to design and print a MPP-based silencer tuned to have peak TL at 3500 Hz. This particular frequency is the blade passage frequency dominating the noise of a typical turbocharger.

Three MPP options with suitable parameters were designed using the VA One software [14] “perforate” type of Noise Control Treatment (NCT) [15] together with the Design Optimization module.

Diameter of the holes and area ratio were constrained. Then, suitable panel thicknesses and cavity depths were sought for the target tuning frequency of 3500 Hz. At the tuning frequency, mass-spring resonance of the air volumes in the holes (mass) and backing cavity (spring) takes place. The number of designs producing the desired tuning frequency is very large. Three MPP-gap options with reasonable panel thicknesses and cavity depths were chosen for further study. These are listed in Table 1.

4. Samples for Impedance Measurement and Hole Analysis

Since the holes in options A and B are relatively small, it was decided first to manufacture suitable samples for subsequent hole analysis and impedance measurement. The samples were printed with a 3D Systems ProJet 6000 HD using 0.05 mm layer thickness and are shown in Figure 4. The material is UV-curable plastic called “Visijet SL Impact”. The density of the material is 1.18 g/cm³ and its Young’s modulus is 2626 MPa. The cup-like shape was chosen in order to ensure that the sample stays in the correct place and position in the impedance tube. The outer diameter of the samples is 34.8 mm.

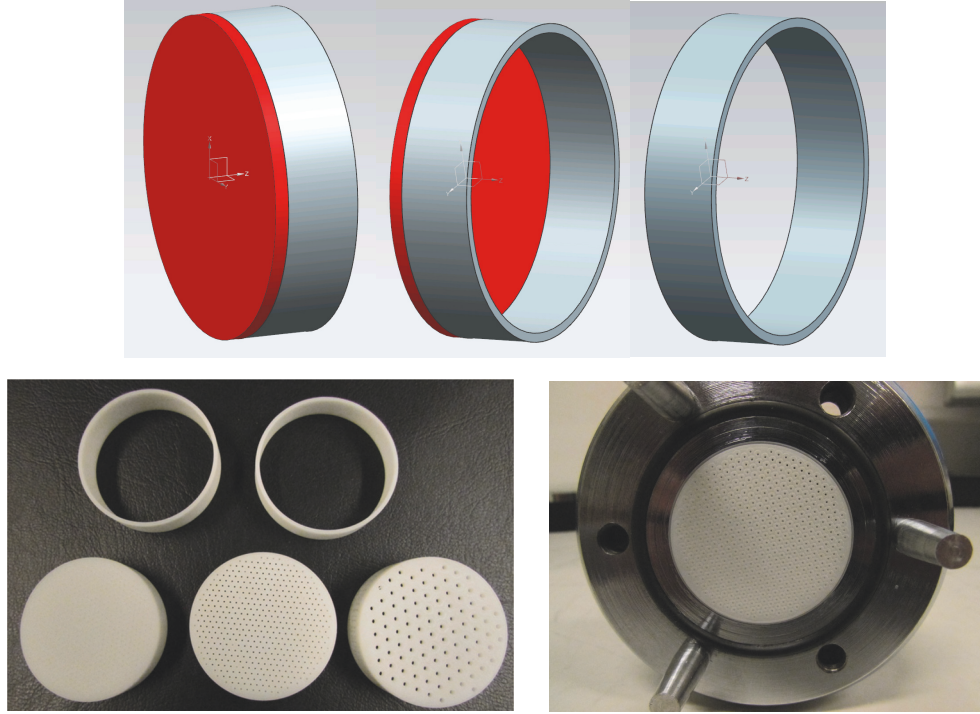


FIGURE 4: MPP samples for impedance measurements. Top: CAD figures. Bottom left: printed samples; bottom right: a sample installed in the impedance tube.

5. Hole Analysis

As the additively manufactured test pieces are not perfect, microscopic photographs of the samples were taken and the holes were analysed statistically using the images. For the MPPs, open area ratio has significant effect on the acoustic properties. Area of the holes was determined using image analysis and histograms of equivalent diameters were plotted (Figure 5).

The results show that 1.0 mm holes of the option C were very accurate, whereas 0.3 and 0.4 mm holes of options A and B were, on the average, smaller than target. Accuracy of the 0.4 mm holes (B) is still relatively good, but diameters of 0.3 mm holes (A) are quite widely distributed around 0.24 and 0.3 mm. There are also quite many very small (i.e., practically closed) holes in option A.

6. Impedance Measurements and Results

ACUPRO Tube [16, 17] was used in impedance measurements. The principle of impedance measurement utilizes the two-microphone transfer function described in standards ASTM E1050-95 and ISO 10534-2. The upper frequency limit of the system is approximately 5600 Hz, but impedance curves start to show irregularity slightly above 5000 Hz.

The measured impedance quantity is the ratio of sound pressure and particle velocity at the surface of interest. The rigorous name of the quantity is “normal specific acoustic

impedance”. The phrase “normal” refers to the direction of the incoming wave and “specific” tells that particle velocity is used (instead of volume velocity). Normalized impedance means impedance divided by the characteristic impedance of the air, $z_0 = \rho c_0$. The term used here is “impedance” meaning the normalized value unless stated otherwise.

The measured results for samples at frequency range 2000 to 5000 Hz are displayed in Figure 6. For option B and C samples the tuning frequency seems to be approximately correct. This is seen from the imaginary part changing sign at 3500 Hz.

In the option A sample, the frequency is approximately 3000 Hz. There is local peak in the real part at 2500 Hz (A) or 3500 Hz (B and C). This comes, presumably, from the elastic resonances in the sample.

7. Silencers

The overall structure of the MPP silencer is shown in Figure 7. The silencer is divided circumferentially into six cavities, which are 9.7 mm deep in the radial direction. The axial length of the cavities is 30 mm.

Two versions were printed, as seen in Figure 8. In the long version, there are 8 cavities axially and in the short version there are three cavities. The total length of the silencers is 335 mm and 170 mm, respectively. The total length of the MPP section is 265 and 100 mm, respectively. The inner diameter

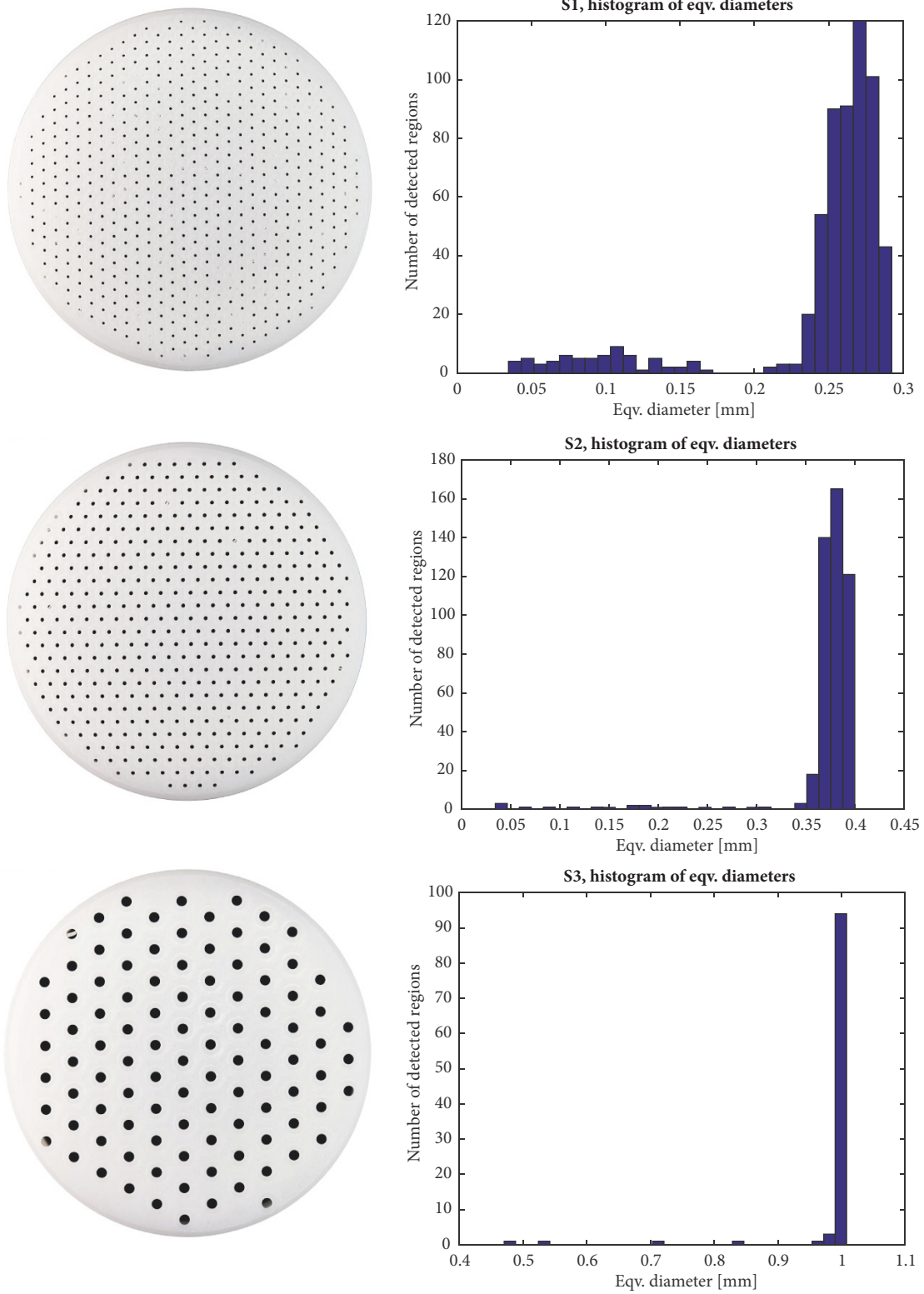


FIGURE 5: Image analysis of MPP impedance samples. Top to bottom: A (0.3 mm), B (0.4 mm), and C (1.0 mm holes). Diameter histograms on the right.

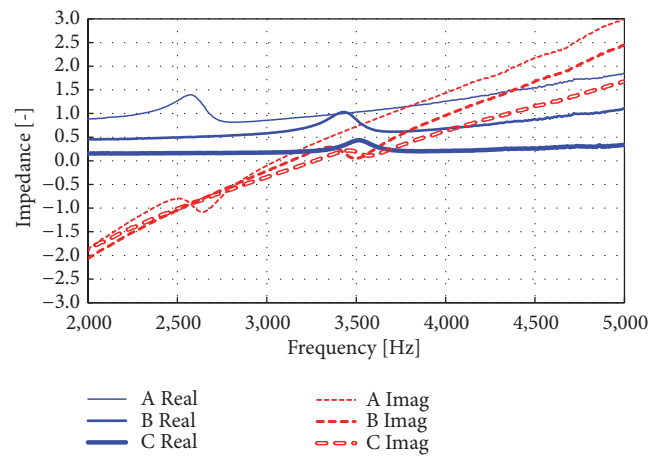


FIGURE 6: Measured real and imaginary parts of impedances of MPP samples A, B, and C.

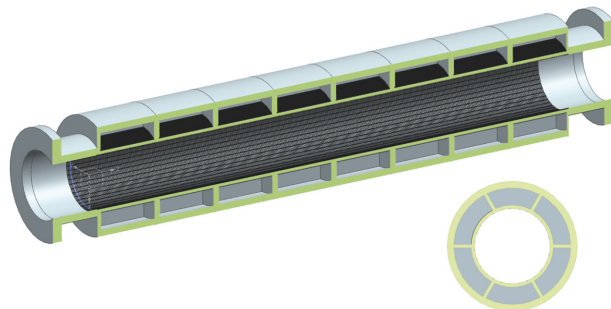


FIGURE 7: Silencer structure, long version.

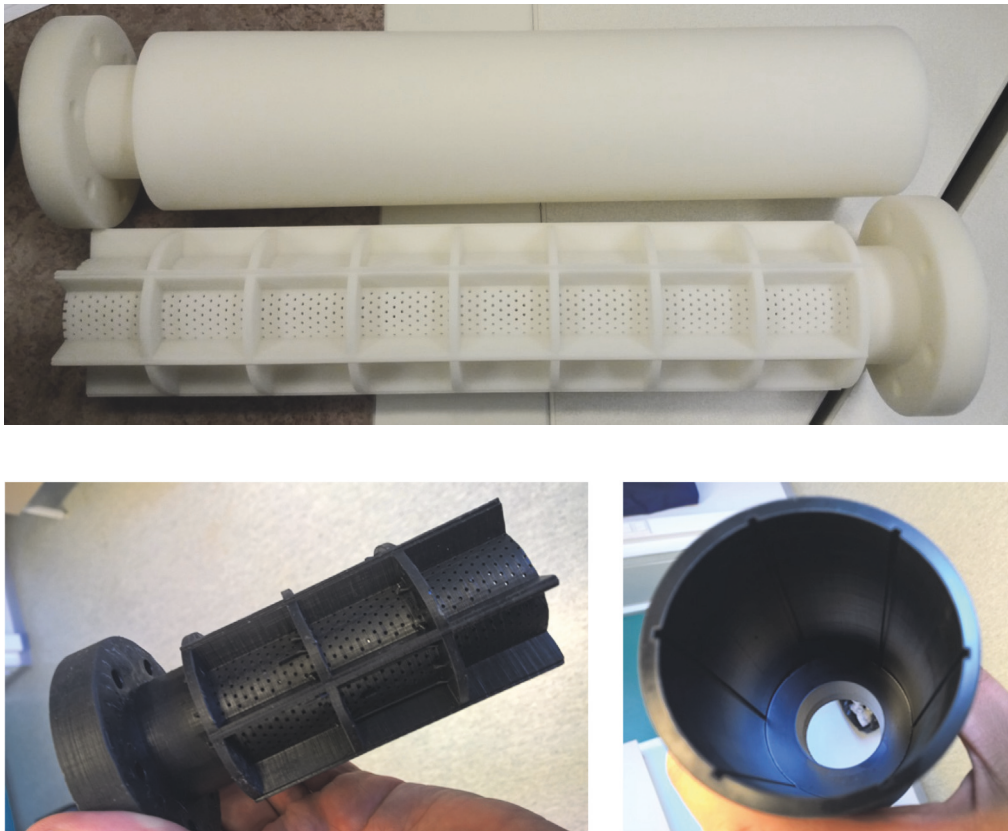


FIGURE 8: Long and short silencer versions. Bottom figure shows grooves for assembling the parts tightly together.

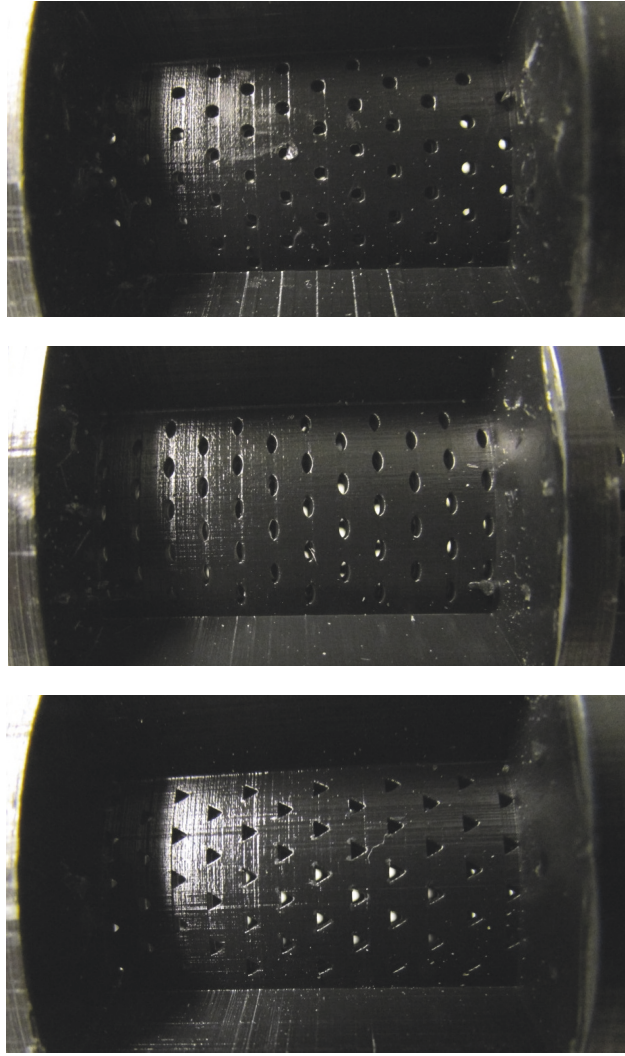


FIGURE 9: Top: option C circular holes; middle: eye-shaped holes; bottom: triangular holes. Perforation ratio is 10% and the material thickness is 1.5 mm for all variants.

of the passage equals to the inner diameter of the TL tube, 34.8 mm.

Only the option C MPP was used in silencers. Options A and B were omitted at this point, because of apparent difficulties to print the holes accurately. Another reason was that equation (2) indicates the optimal value for real part of impedance at 3500 Hz and $R=0.0174$ m to be approx. 0.31. The measured values were 1.03, 0.87, and 0.43 for samples of options A, B, and C, respectively; see Table 2. Thus, options A and B were judged to have too high resistance. In fact, they are more suitable to modal filter silencers. Measured real parts of impedances were systematically 2 to 4 times higher than those predicted.

Material of the long silencer is the same as the impedance samples. The short version of the silencer was printed with a Formlabs Form 2 SLA printer using the Formlabs black photoreactive resin and layer thickness of 0.025 mm. Young's modulus is 1600 MPa after printing and 2800 MPa postcured but can vary depending on layer thickness.

8. Special Hole Types

As 3D-printing is not limited to circular hole shapes, two other hole types were printed and investigated for short silencer versions. These are the following:

- (i) Eye-shaped holes, same hole area and area ratio as option C. Hole dimensions are approx. length 1.66 mm and width 0.67 mm.
- (ii) Triangular holes, same hole area and area ratio as option C. Hole side length is ca. 1.35 mm.

These hole types are shown in Figure 9 together with circular holes.

9. TL Measurements

An ACUPRO Tube [16, 17] fitted for transmission loss measurements was used as seen in Figure 10. The TL measurement is based on determination of the transfer matrix

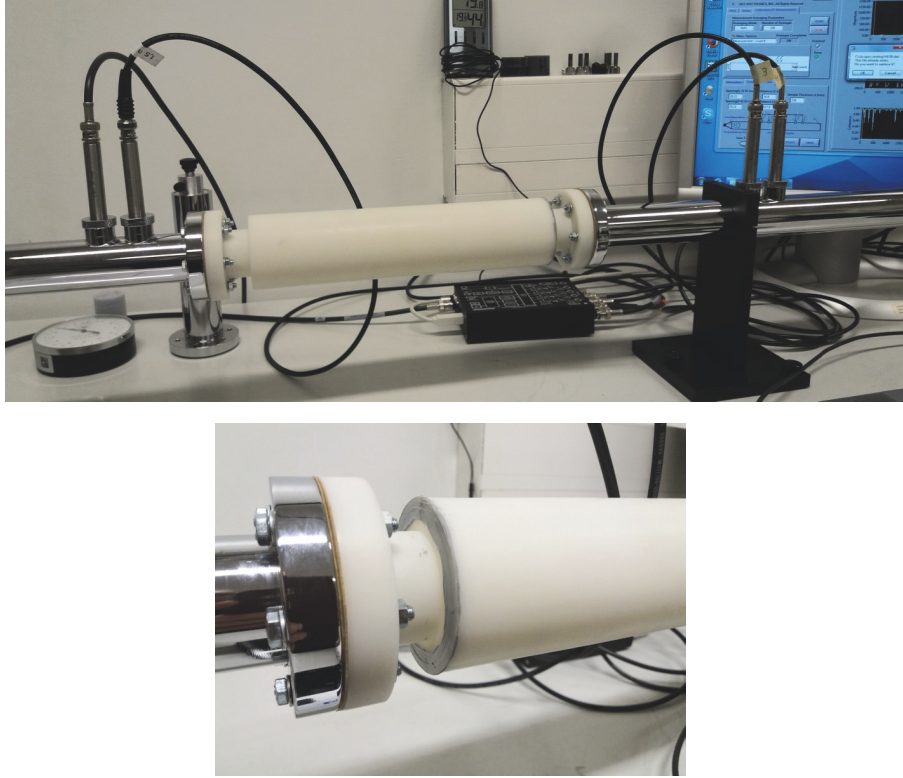


FIGURE 10: Long silencer version in measurements. Bottom figure shows the sealed junction between the outer and inner parts.

TABLE 2: Measured impedances of the three MPP-gap options at 3500 Hz compared to optimal value.

Option	Measured		VA One prediction using theory in [15]	
	Real Part	Imaginary part	Real Part	Imaginary part
A	1.03	0.73	0.46	0.08
B	0.87	0.048	0.33	0.09
C	0.43	0.18	0.10	0.028
Optimum according to equation (2) for $R=0.0174$ m at 3500 Hz				
	Real Part		Imaginary part	
	0.31		-0.13	

using the two-load method in the plane wave frequency range of the tube. For the 34.8 mm tube, the practical upper frequency limit is approximately 5500 Hz. As in the impedance measurements of the hole samples, the TL curves start to show irregularity soon after 5000 Hz. The upper limit of measurable TL is not specified, but, evidently it is not more than approximately 60 dB. The highest measured TLs shown in the examples within the tube documentation [17] are approx. 40 dB.

10. Simulations and Comparison against Measurements

TL of the silencers was simulated with acoustic FEM within VA One software [14]. Solving the models was done in modal coordinates. Calculation of TL is based on the hybrid

method [18–20] using a diffuse acoustic field (DAF) as the pressure excitation. DAF is a rain-on-roof type random load without spatial correlation between various on excited surface. The impedance matrices needed for general anechoic terminations are created using acoustic spectral element techniques applied at the termination surface meshes. Inlet and outlet extensions were included in the models to ensure plane wave conditions at the actual location of the MPP part. Basic setting of the models is depicted in Figure 11.

Two different types of models were created for both the short and long silencer versions. In the first type, the MPP surface and backing cavity were modelled using the impedance measured from sample C. The impedance was inserted into the model as numeric data for a 1x1 FE Area Junction (boundary condition), located on the MPP surface of the silencer passage.

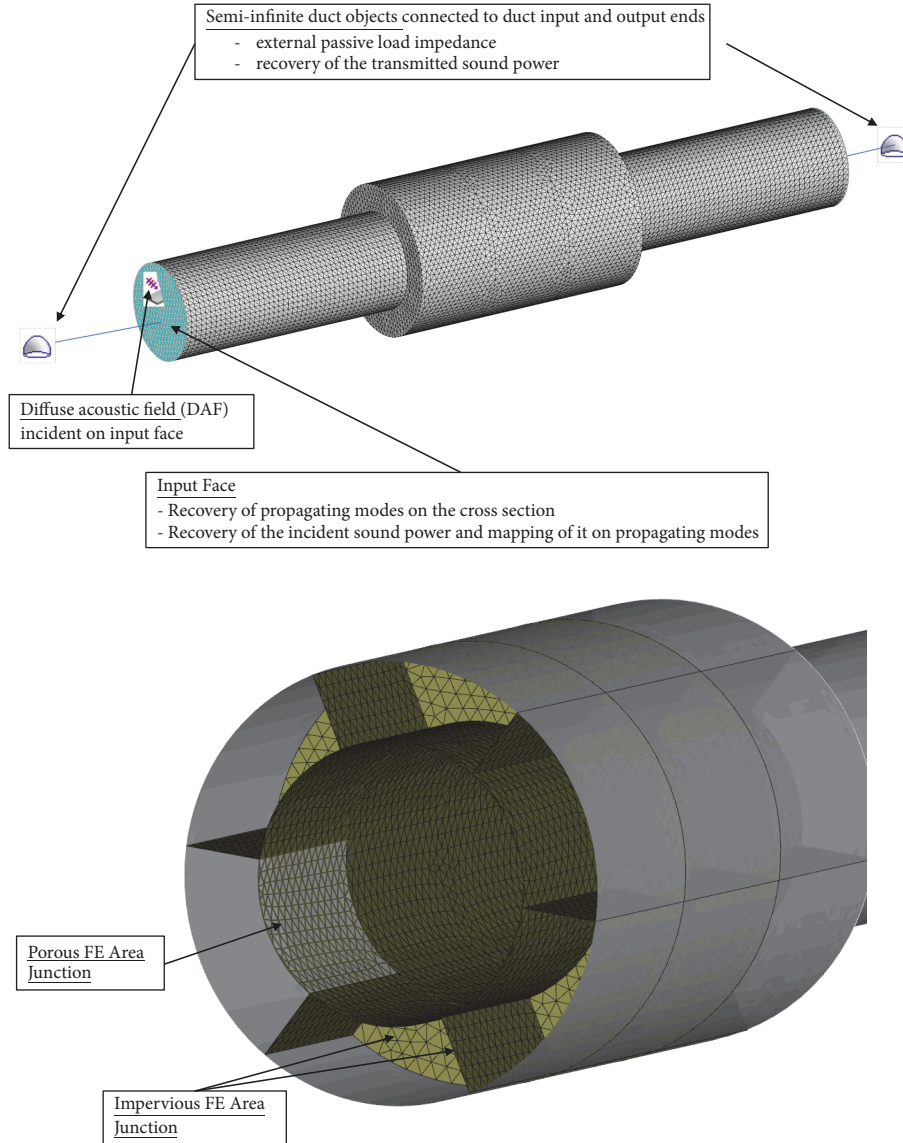


FIGURE 11: Setting of a VA One model for TL calculation and FE Area Junction types in models with explicit cavities.

In the second type of models, the cavities were modelled explicitly. Then the MPP was modelled as a 2x2 transfer impedance of the area junctions between the duct and cavities. The transfer impedance is based on the Bauer perforate model [21] for circular holes. The models are solved up to 6 kHz in modal coordinates using modes up to 16 kHz.

The models are depicted in Figure 12. Selected model data is in Table 3.

Comparison of measured and simulated values of TL is in Figure 13.

In short version, maximum value of simulated TL is considerably higher than maximum value of measured TL. In long version, maximum values of simulated and measured TLs agree better. In both versions, bandwidth of simulated TL is considerable higher than bandwidth of measured TL. The nominal tuning frequency 3500 Hz is quite well in the middle of TL band.

Reasons for these differences include leaks between backing cavities, uncertainties in impedance and structure-borne sound. TLs above 60 dB seen in simulation results are speculative, because of the limited dynamic range of the apparatus. The coherence around tuning frequency was very low in case of the long version.

11. Effect of Hole Shape on TL

TL of short silencers with different hole versions is in Figure 14. There is no significant difference in TL of silencer with different hole types. Because of the relatively large holes, the possible difference in resistive component of the impedance does not have significant effect on the performance. The mass reactance of the holes with same hole cross-sectional area, perforation ratio, and material thickness is the same and leads to same tuning frequency and TL.

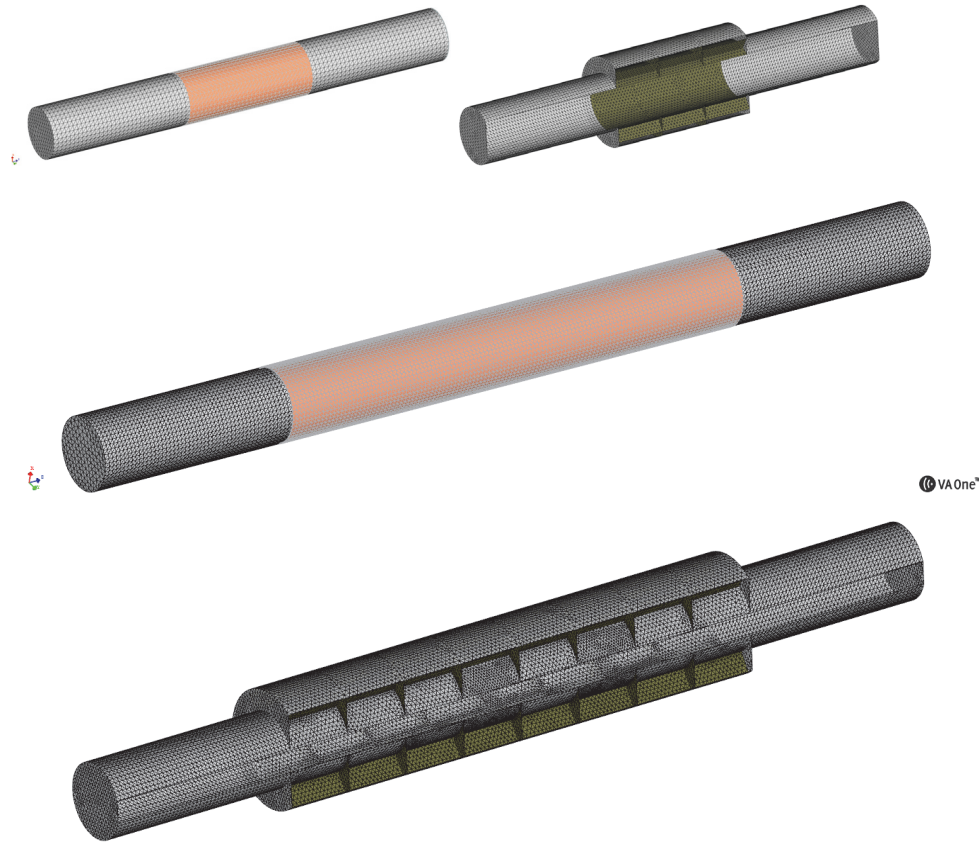


FIGURE 12: Acoustic FE models. Models using the given impedance boundary condition are on the top left and in the middle. Models with explicit cavities are on the top right and on the bottom.

TABLE 3: Selected model data. Typical element size in the models is 1-2 mm.

Model	Number of nodes	Number of elements	Number of eigenmodes below 16 kHz
Short, Local reaction	7577	31892	174
Short, Explicit cavities	45977	211728	299
Long, Local reaction	27141	123529	261
Long, Explicit cavities	102110	457621	624

12. Conclusions and Future Work

MPP-based silencers tuned to have peak TL at 3500 Hz were successfully realised using 3D-printing (additive manufacturing).

Three different circular hole options (A, B, and C) of MPP, combined with a suitable backing cavities tuned to 3500 Hz, were designed. These options had target hole diameters of 0.3, 0.4, and 1.0 mm and perforation ratios of 5, 7, and 10 %, respectively. Acoustic impedance measurements showed that quite accurate tuning was achieved with all options (imaginary part changed sign at 3000-3500 Hz range).

The image analysis of the MPP samples showed that the holes of options A and B were, on the average, approx. 0.275 and 0.375 mm compared to targeted 0.3 and 0.4 mm. The shapes of the holes deviated from the round shape. The 1.0 mm holes of the option C sample were far more accurate.

A long and a short version of a MPP silencer with option C holes were printed. The TL measured for the long version was 50...60 dB in the targeted frequency range. In fact, the maximum of TL could not be measured accurately due to poor signal to noise ratio downstream of the silencer. The short version showed TL of approx. 30...35 dB at the tuning frequency.

Two other short versions with the same hole area and area ratio than option C were printed. These were versions with eye-shaped holes and with triangular holes. The performance of these was similar with the performance of the option C. This is because in relatively large holes, reactance is the dominating component of the impedance. Then the different shapes of holes having the same area have no effect.

Two different types of acoustic FE models were created for both the short and long silencer versions. In first type,

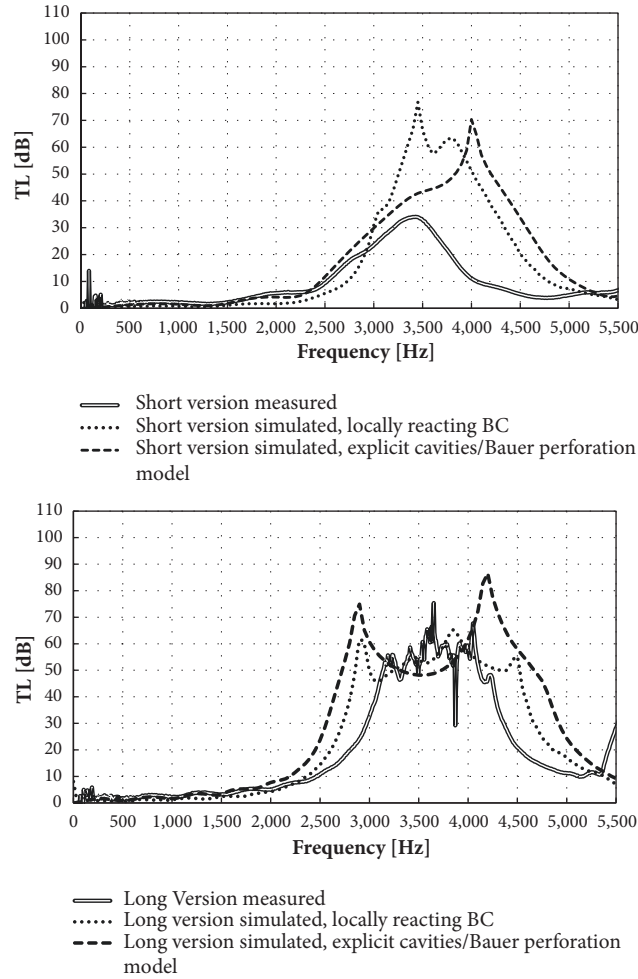


FIGURE 13: TL results for circular holes.

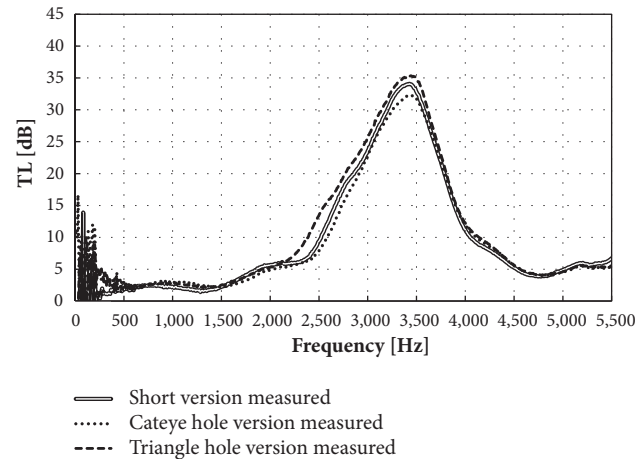


FIGURE 14: TL results for circular, cateye, and triangular holes, short silencer version.

the MPP surface and backing cavity were modelled using the measured impedance of option C sample. The impedance was inserted into the model as numeric data for a 1x1 FE Area Junction (boundary condition), located on the MPP surface of the silencer passage. In the second type of model,

the cavities were modelled explicitly. Then the MPP was modelled as a 2x2 transfer impedance of the area junctions between the duct and cavities.

In the short version, maximum value of simulated TL was considerably higher than maximum value of measured TL.

In long version, maximum values of simulated and measured TLs agree better. In both versions, bandwidth of simulated TL is considerable higher than bandwidth of measured TL. The nominal tuning frequency 3500 Hz is quite well in the middle of simulated TL band. Reasons for these differences include leaks between backing cavities, and structure-borne sound. TLs above 60 dB seen in simulation results are speculative, because of the limited dynamic range of the apparatus.

There is no clear superiority between the two types of acoustic FE models. Both types gave useful results, but the accuracy was only approximate. The limitations in both were the exclusion of structural propagation and leaking between cavities. The limitation of the first type of model is the assumption of pure local reaction given as predefined boundary condition. The limitation of the second type of models is probably the accuracy of the perforation theory used.

3D-printing has many advantages in concept development of small scale ducted silencers. These include the following: (1) printing is very fast compared to any other manufacturing method, (2) there are no limitations to shape, and (3) the overall accuracy is good. The main limiting factor noticed in the special context of MPP-based silencers is the printing of very small holes (i.e., below 0.5 mm, say).

There are several possibilities for the next steps, including, but not limited to, (a) effect of simplifying the backing cavity structure (less ribs, axially longer cavities), (b) printing of larger silencers for the TL-tube, (d) development of modular structure for silencer with annular passage, and (e) issues in FE-modelling: plane wave, diffuse and other types of excitation on prediction results.

Data Availability

The data used to support the findings of this study are available from the corresponding author upon request.

Conflicts of Interest

The authors declare that there are no conflicts of interest regarding the publication of this paper.

Acknowledgments

This work has been supported by Wärtsilä Finland Ltd Energy Solutions and VTT Technical Research Centre of Finland Ltd.

References

- [1] D. Maa, "Potential of microperforated panel absorber," *The Journal of the Acoustical Society of America*, vol. 104, no. 5, pp. 2861–2866, 1998.
- [2] H. V. Fuchs, "Chapter 9: microperforated absorbers," in *Applied Acoustics: Concepts, Absorbers, and Silencers for Acoustical Comfort and Noise Control*, p. 593, Springer Berlin Heidelberg, Berlin, Heidelberg, 2013.
- [3] S. Sack and M. Åbom, "Modal filters for mitigation of in-duct sound," in *Proceedings of the 172nd Meeting of the Acoustical Society of America*, p. 040004, Honolulu, Hawaii, 2016.
- [4] S. Sack and M. Åbom, "Modal filters for in-duct sound based on the cremer impedance and micro-perforated plates," in *Proceedings of the 45th International Congress and Exposition on Noise Control Engineering: Towards a Quieter Future, INTER-NOISE 2016*, pp. 3215–3222, Germany, August 2016.
- [5] S. Allam and M. Åbom, "Dissipative silencers based on micro-perforated plates," in *Proceedings of the 11th International Conference on Engines Vehicles (13ICE)*, Capri, Napoli (Italy), Sept 2013, Paper 13ICE-0289. 4p.
- [6] S. Allam and M. Åbom, "A new type of muffler based on microperforated tubes," *Journal of Vibration and Acoustics*, vol. 133, no. 3, pp. 31005–31005-8, 2011.
- [7] R. Kabral, L. Du, and M. Åbom, "Optimum sound attenuation in flow ducts based on the "exact" Cremer impedance," *Acta Acustica united with Acustica*, vol. 102, no. 5, pp. 851–860, 2016.
- [8] J. Yang, "An Experimental and Numerical Investigation on Acoustic Liners with Drainage Slots. ICSV25," *Hiroshima*, vol. 8, pp. 8–12, 2018.
- [9] S. Allam and M. Åbom, "Fan noise control using microperforated splitter silencers," *Journal of Vibration and Acoustics*, vol. 136, no. 3, 2014.
- [10] R. Kabral, L. Du, M. Åbom, and M. Knuttson, "A compact silencer for the control of compressor noise," *SAE International Journal of Engines*, vol. 7, no. 3, pp. 1272–1278, 2014.
- [11] Z. Liu, J. Zhan, M. Fard, and J. L. Davy, "Acoustic properties of multilayer sound absorbers with a 3D printed micro-perforated panel," *Applied Acoustics*, vol. 121, pp. 25–32, 2017.
- [12] L. Cremer, "Theory regarding the attenuation of sound transmitted by air in a rectangular duct with an absorbing wall, and the maximum attenuation constant produced during this process," *Acustica*, vol. 3, pp. 249–263, 1953.
- [13] B. J. Tester, "The optimization of modal sound attenuation in ducts, in the absence of mean flow," *Topics in Catalysis*, vol. 27, no. 4, pp. 477–513, 1973.
- [14] *VA One version 2017*, vol. 1, ESI Group, 2017.
- [15] N. Atalla and F. Sgard, "Modeling of perforated plates and screens using rigid frame porous models," *Journal of Sound and Vibration*, vol. 303, no. 1-2, pp. 195–208, 2007.
- [16] <http://spectronics.net/products/acupro.html>.
- [17] *ACUPRO Version 4.5 manual*, Spectronics, Inc., 2017.
- [18] P. J. Shorter and R. S. Langley, "Vibro-acoustic analysis of complex systems," *Journal of Sound and Vibration*, vol. 288, no. 3, pp. 669–699, 2005.
- [19] P. J. Shorter and R. S. Langley, "On the reciprocity relationship between direct field radiation and diffuse reverberant loading," *The Journal of the Acoustical Society of America*, vol. 117, no. 1, pp. 85–95, 2005.
- [20] V. Cotoni, A. Gallet, F. Guerville, and M. Glessner, "Predicting the acoustic performance of lined ducts across a broad frequency range," in *Inter-Noise 2012*, p. 11, New York, NY, USA, 2012.
- [21] A. B. Bauer, "Impedance theory and measurements on porous acoustic liners," *Journal of Aircraft*, vol. 14, no. 8, pp. 720–728, 1977.

